

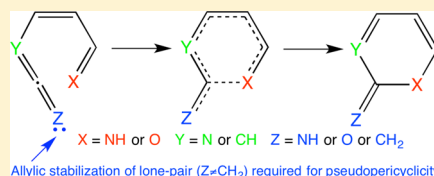
CASSCF Computational Study of Pseudopericyclic Character in Electrocyclic Rearrangements Involving Heteroatoms

Irena R. Bierzynski,[†] Cassandra A. Settle,[†] Henry W. Kreiman,[†] and James A. Duncan*

Department of Chemistry, Lewis & Clark College, Portland, Oregon 97219-7899, United States

Supporting Information

ABSTRACT: The Complete Active Space Self-Consistent Field (CASSCF) computational method, with the 6-31G* basis set, was used to examine six electrocyclic rearrangements, each involving a 1,2,4,6-heptatetraene skeleton with two variously located oxygen and/or nitrogen heteroatoms, as a way to determine which, if any, are pseudopericyclic as opposed to pericyclic. Primarily through the close examination of the active space orbitals, but also considering transition structure geometries and activation energies, it was concluded that rearrangements $3 \rightarrow 4$, $5 \rightarrow 6$, $7 \rightarrow 8$, and $9 \rightarrow 10$ are pseudopericyclic with two orbital disconnections each, whereas the $13 \rightarrow 14$ and $15 \rightarrow 16$ rearrangements are pericyclic. Our conclusions agreed with those of others in two of the four cases that had been studied previously by density functional theory ($3 \rightarrow 4$ and $7 \rightarrow 8$) but ran contrary to the previous conclusions that the $5 \rightarrow 6$ rearrangement is pericyclic and that the $15 \rightarrow 16$ rearrangement is pseudopericyclic. Our results are also compared and contrasted to previous similar ones of ours involving the $3 \rightarrow 4$ electrocyclization (essentially pericyclic), the $11 \rightarrow 12$ [3,3] sigmatropic rearrangement (pseudopericyclic), and similar [3,3] sigmatropic rearrangements (all pericyclic), and detailed rationales for these latest results are provided.



INTRODUCTION

Pericyclic reactions are among the most important of all chemical reactions.¹ Indeed: "Some of the most elegant and insightful mechanistic studies ever executed were designed to probe pericyclic reactions."² By definition, pericyclic transition states are composed of a cyclic array of atoms and an associated cyclic array of interacting orbitals that have no disconnections among them. Classified as electrocyclizations, sigmatropic rearrangements, cycloadditions, cheletropic, and group transfers; many pericyclic reactions³ are highly stereoselective in accordance with the Woodward–Hoffmann (W–H) rule⁴ that is well grounded in molecular orbital theory. The W–H rule can also predict which pericyclic reactions are likely to occur ("allowed") or unlikely to occur ("forbidden").⁴ All types of pericyclic reactions have been utilized in organic synthesis,^{3b–h} especially in the synthesis of heterocycles^{3b} and natural products.^{3c–h}

Eventually though, a new class of important chemical reactions was recognized that appears on first glance to be pericyclic (since their transition states involve a cyclic array of atoms) but on closer inspection appears to have one or more disconnections in the cyclic array of interacting orbitals. These reactions, and their associated transition states, have been termed pseudopericyclic⁵ to reflect the fact that orbital disconnections occur when orbitals orthogonal to bonding orbitals, in the reactant, participate in the formation of new bonds, and are not required to obey the W–H rule. Thus, it is desirable to be able to predict in advance which reactions should be pericyclic and which pseudopericyclic, since the former are more likely to be stereoselective and the latter may always be "allowed".

With the goal to help define those characteristics that make one reaction pericyclic and another pseudopericyclic, and thus perhaps eventually better predict their chemo-, regio-, and stereoselective nature, we have previously studied two of the five types of potentially pseudopericyclic reactions: electrocyclizations⁶ and sigmatropic rearrangements.⁷ This paper reports on our further study of possible pseudopericyclic character in electrocyclic reactions. Electrocyclic reactions are used in the synthesis of many biologically relevant and pharmacologically active molecules, especially those with heterocyclic systems.⁸ In particular, they are involved in the synthesis of antibiotics, steroids, and amino acids, among other compounds, both in the laboratory and within biological systems.^{9,10} They are particularly useful as a way to form new carbon–carbon single bonds, can involve ring opening as well as ring closure, and may be used to control stereochemistry in synthesis, the latter only if they are pericyclic as opposed to pseudopericyclic.

While the distinction between pericyclic and pseudopericyclic rearrangements is related to the behavior of the molecular orbitals (MOs), different characteristics obtained from calculations at the level of density functional theory (DFT) are most often used to distinguish between the two. For example, the level of aromaticity of the transition structures has been addressed using nucleus independent chemical shift (NICS) analysis.¹¹ In addition, the magnetic-based criterion anisotropy of the current-induced density (ACID) has been used to quantify the extent of conjugation along bonds.¹²

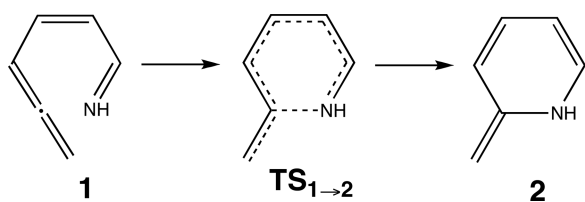
Received: September 22, 2015

Published: December 10, 2015

Another makes use of the electron localization function (ELF) that estimates the relative electron sharing between a particular electron-pair bond and adjacent bonds.¹³ Finally, natural bond orbital (NBO) analysis can demonstrate rotation about bonds in the transition structure.¹⁴

The use of these different methods, along with the emergence of the idea that degrees of pseudopericyclic character may exist in a particular reaction, has led to disagreements in the field. One such disagreement arose over the mechanism of the concerted rearrangement of (*E*)-7-azahepta-1,2,4,6-tetraene (**1**) to 1-aza-6-methylidencyclohexa-2,4-diene (**2**) through transition structure $TS_{1\rightarrow 2}$, as shown in Scheme 1.

Scheme 1. Electrocyclization Whose Mechanism Proved To Be Controversial



This rearrangement provides two opportunities for orbital disconnections among the four possible mechanisms shown in Figure 1. Illustration a depicts a classically pericyclic mechanism; the C–N π -bond is used to make the new σ -bond, along with the inner π -bond of the cumulene system. The mechanism shown in illustration b depicts a pseudopericyclic reaction with one orbital disconnection on the central

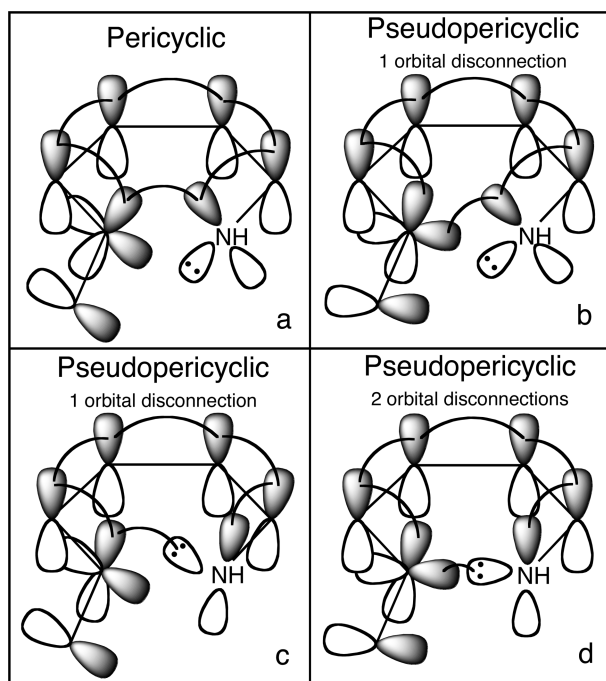


Figure 1. Cartoon representations of the four possible mechanisms for the **1** \rightarrow **2** rearrangement: (a) classically pericyclic mechanism; (b) pseudopericyclic mechanism with an orbital disconnection on the central carbon of the cumulene system; (c) pseudopericyclic mechanism with an orbital disconnection on the nitrogen; (d) pseudopericyclic mechanism with both possible orbital disconnections.

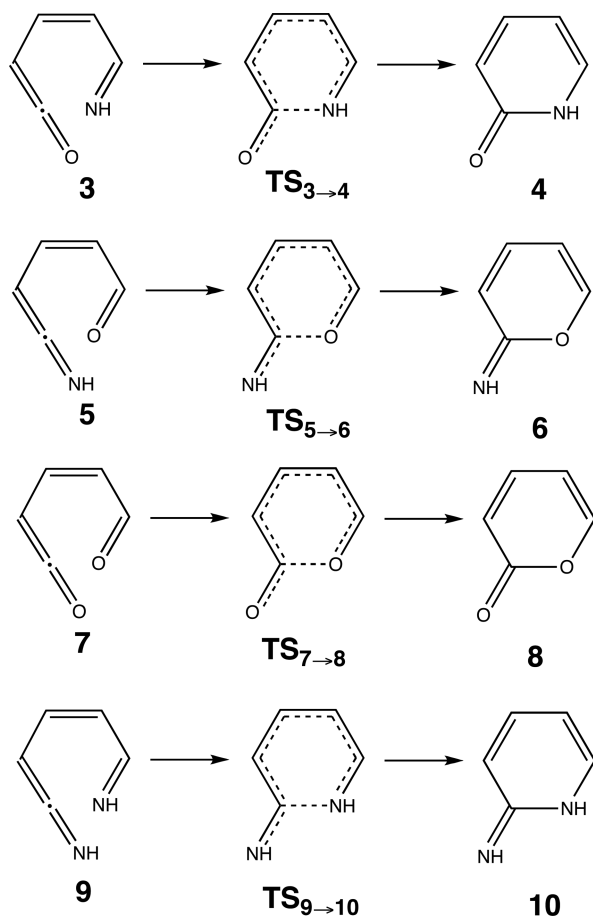
carbon of the cumulene system as the outer π -bond is used to form the new σ -bond. Another possible orbital disconnection, on the nitrogen of the imine group, is shown in c of Figure 1 and illustrates the lone-pair orbital on the nitrogen participating in formation of the new σ -bond, making this possibility also pseudopericyclic with one orbital disconnection. If both the outer π -bond and lone-pair orbital are used, the reaction is pseudopericyclic with two orbital disconnections, as illustrated by d of Figure 1.

This reaction was first studied both experimentally and computationally by de Lera and Cossío, who primarily used NICS and NBO methods to conclude that $TS_{1\rightarrow 2}$ has pseudopericyclic character.¹⁵ However, Rodríguez-Otero et al. later reported on results of further NBO calculations applied to this rearrangement that led them to question this conclusion. They argued that the electrocyclization is “essentially pericyclic,” though “assisted” by the lone-pair orbital on nitrogen.¹⁴ Both groups stood by their initial claims in subsequent discussions of the issue.^{16,17} In addition, Chamorro et al. reported on ELF results they claimed supported Rodríguez-Otero’s conclusion that the rearrangement is pericyclic,^{18,19} whereas Solà and Poater claimed their own ELF results supported de Lera and Cossío’s initial interpretation that it is pseudopericyclic.^{13,20}

Taking another approach, we studied the **1** \rightarrow **2** rearrangement using the Complete Active Space Self-Consistent Field (CASSCF) method.⁶ (Previously, Houk et al. used the CASSCF method to study the electrocyclic ring opening of cyclobutenes²¹ and recently the reactions of allenes as dienophiles in the Diels–Alder reaction as well.²²) The “active space” selected consisted of the localized molecular orbitals that may potentially be involved in the reaction. For example, in the case of the **1** \rightarrow **2** rearrangement it is necessary to include the electrons in the lone-pair orbital on the nitrogen atom in order to determine whether or not they affect the mechanism of the reaction. Our results more closely conformed to those obtained by Rodríguez-Otero, as opposed to those obtained by de Lera and Cossío, though we found the effect of the lone pair to be significant enough to warrant the term “secondary orbital effect,” since it appears to overlap with the new σ -bond in the transition structure.⁶ However, the C–N and C–C π -bonds were shown as primarily participating in the formation of the new σ -bond. The calculated transition structure most resembles illustration a of Figure 1, so the **1** \rightarrow **2** rearrangement is not a pseudopericyclic reaction.

Some additional electrocyclic rearrangements, the top three in Scheme 2, have been studied computationally by Rodríguez-Otero et al., all with DFT methods. They analyzed $TS_{5\rightarrow 6}$ and $TS_{7\rightarrow 8}$ using both NBO and NICS methods and concluded that $TS_{5\rightarrow 6}$ was pericyclic²³ whereas $TS_{7\rightarrow 8}$ was pseudopericyclic.¹³ The same conclusion was reached by Birney for $TS_{7\rightarrow 8}$.²⁴ Rodríguez-Otero et al. were unable to locate $TS_{3\rightarrow 4}$ but concluded that the **3** \rightarrow **4** rearrangement is pseudopericyclic, based on the positioning of the lone pair in a reacting conformation.²⁵

These results are at least consistent with the proposition, espoused by some,^{7,24,25} that increased electrophilicity at the central carbon atom of the cumulene (C2 in Figure 2, structure a), due to the presence of an electronegative atom at position 1 or 3 of Figure 2, structure a, and/or the increased nucleophilicity of the heteroatom at position 7 (cf. Figure 2, structure a), should contribute to pseudopericyclic character in the rearrangement.

Scheme 2. Four of the Electrocyclic Rearrangements Studied in the Current Investigation^a

^aThe first three have been studied previously with DFT methods. Of these, only 7 → 8 was concluded to be pseudopericyclic. Rearrangement 5 → 6 was concluded to be pericyclic, and 3 → 4 returned ambiguous results.

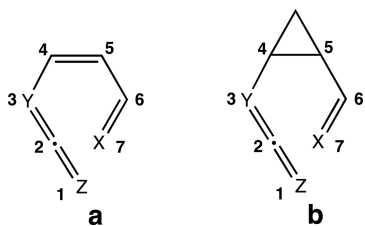
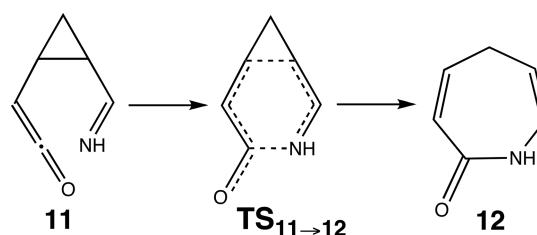


Figure 2. Generalized ChemDraw structures of a heteroatom-containing 1,2,4,6-heptatetraene (a) and a heteroatom-containing *cis*-disubstituted cyclopropane (b). Numbers have been included in order to reference equivalent positions in distinct molecules.

We recently considered the electrophilicity/nucleophilicity concept discussed above as part of a CASSCF study of a series of seven [3,3] sigmatropic rearrangements involving 1,2-disubstituted cyclopropane reactants containing various heteroatoms (cf. Figure 2, structure b).⁷

Only one of the seven rearrangements, namely that of *cis*-1-iminyl-2-ketenylcyclopropane (11) to amide 12, as shown in Scheme 3, proved to be pseudopericyclic. This conclusion was based on the appearance of the active-space orbitals in TS_{11→12} and its close-to-planar six-membered ring geometry. The six other transition structures, which had differently placed oxygen

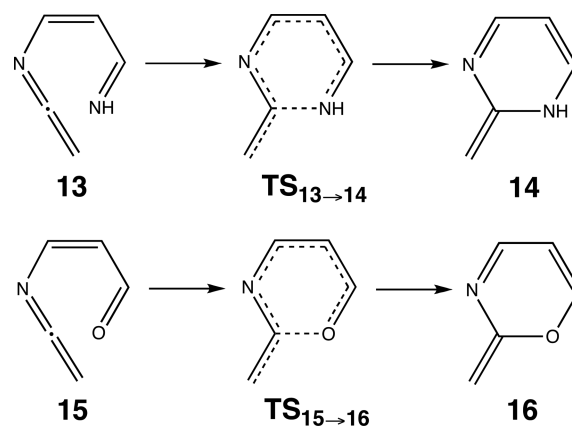
Scheme 3. [3,3] Sigmatropic Rearrangement Determined by CASSCF Methods To Be Pseudopericyclic



and nitrogen heteroatoms, were boat-shaped, and five of them were pericyclic based on the appearance of their active-space orbitals. (The other one gave an ambiguous result.) Indeed, of all the reactants, 11 has the most nucleophilic heteroatom (nitrogen) in the position corresponding to 7 in Figure 2, structure b and the most electrophilic carbon atom in the position corresponding to 2 in Figure 2, structure b, due to the adjacent oxygen atom. This result supports the idea, discussed above, that these factors should increase the likelihood of pseudopericyclic character. In addition, we also suggested that the formation of an allyl system in TS_{11→12}, involving a lone pair on the oxygen atom, may help stabilize this particular pseudopericyclic transition structure.⁷

The current study uses the CASSCF method we applied to the 1 → 2 rearrangement (Scheme 1) with a single heteroatom (nitrogen) to examine six additional rearrangements involving two nitrogen and/or oxygen heteroatoms each. These include the 3 → 4, 5 → 6, and 7 → 8 rearrangements studied by others with DFT methods^{17,23–25} as well as the 9 → 10 rearrangement, as shown in Scheme 2. The other two rearrangements studied (13 → 14 and 15 → 16) are shown in Scheme 4. The

Scheme 4. Additional Electrocyclic Rearrangements Selected for CASSCF Computational Investigation



15 → 16 rearrangement has also been studied by Rodríguez-Otero et al. using NBO, NICS, and ACID techniques, and it was concluded that it is pseudopericyclic,²³ the same conclusion reached for the 3 → 4 and 7 → 8 rearrangements.

Based upon the results of our study of the 11 → 12 [3,3] sigmatropic rearrangement, one might expect the 3 → 4 electrocyclic rearrangement to be most likely to exhibit pseudopericyclic character because it has the most nucleophilic heteroatom (nitrogen) in the nucleophilic position and the most electrophilic central carbon atom of the cumulene system, due to the oxygen atom, at the end. Conversely, one might

expect rearrangement $5 \rightarrow 6$ to be the least likely to exhibit pseudopericyclic character since it has the weakest nucleophilic heteroatom (oxygen) and the least electronegative heteroatom in the cumulene system (nitrogen). If the rearrangements vary in their degrees of pseudopericyclic character, one or more calculated transition structures may have characteristics that demonstrate a mixture of the possible pseudopericyclic and pericyclic transition structures for that rearrangement.²⁶

Our impetus for studying, in addition, the two rearrangements shown in Scheme 4 stemmed from our contention that the formation of a stabilizing allyl system in $TS_{11 \rightarrow 12}$ was at least partially responsible for its observed pseudopericyclic character. All four rearrangements shown in Scheme 2 can take advantage of this, whereas the two rearrangements in Scheme 4 cannot since they have no heteroatom with a lone pair of electrons on the terminus of the cumulene.

Studying these reactions changes only the effect of the allyl system because the nitrogen atom is still adjacent to the central carbon atom of the cumulene. Thus, the electrophilicity of the center carbon atom remains essentially the same.

COMPUTATIONAL METHODS

All stationary points were optimized at the CASSCF/6-31G* level using Gaussian 03^{27a} or Gaussian 09.^{27b} All structures were obtained using a (12,10) active space, i.e., 12 electrons in 10 orbitals. The 12 electrons in the active spaces of the reactants and transition structures include the eight π -electrons of the four double bonds, two electrons in a lone pair on one nitrogen/oxygen atom, and two electrons in a lone pair on the other nitrogen/oxygen atom. The 12 electrons in the active spaces of the products include the six π -electrons of the three double bonds, two electrons in a lone pair on one nitrogen/oxygen atom, two electrons in a lone pair on the other nitrogen/oxygen atom, and the two electrons of the new σ -bond. Dynamic electron correlation was included by running single-point CASPT2/6-31G* calculations on CASSCF/6-31G* stationary points using Molcas 7.4.²⁸

Frequency calculations were performed on all structures to obtain zero-point corrected energies. Frequency calculations were also used to verify concerted transition structures. The single imaginary (negative) frequency for each transition structure was animated to confirm that the correct bond was forming. Intrinsic reaction coordinate (IRC) calculations were also performed to confirm that the calculated transition structures were on the correct potential energy surfaces between the desired reactants and products. Three-dimensional structural representations, including molecular orbital representations (with the contour value routinely set to between 0.07 and 0.10) and normal mode vectors, including those in Supporting Information, were generated using MacMolPlt²⁹ except for Figure 5, which was generated with GaussView 5.0.³⁰

RESULTS AND DISCUSSION

CASSCF calculations show that the $3 \rightarrow 4$ rearrangement (Scheme 2) is pseudopericyclic as concluded by Rodríguez-Otero et al., even though they were unable to locate a transition structure.²⁵ In particular, it is shown to have two orbital disconnections (cf. illustration d of Figure 1). Figure 3 shows selected active-space molecular orbitals calculated for our transition structure of this rearrangement ($TS_{3 \rightarrow 4}$) and in b the lone-pair orbital of the nitrogen atom can be clearly seen participating in the formation of the new σ -bond. [A full set of active-space orbitals for the reactants, products (except 4^{31}), and transition structures of all electrocyclizations studied is provided in the Supporting Information.] The external π -orbital of the ketenyl ($-\text{CH}=\text{C}=\text{O}$) system can also be seen participating in formation of the σ -bond. This conclusion is reinforced by the orbitals represented in a and c of Figure 3. In

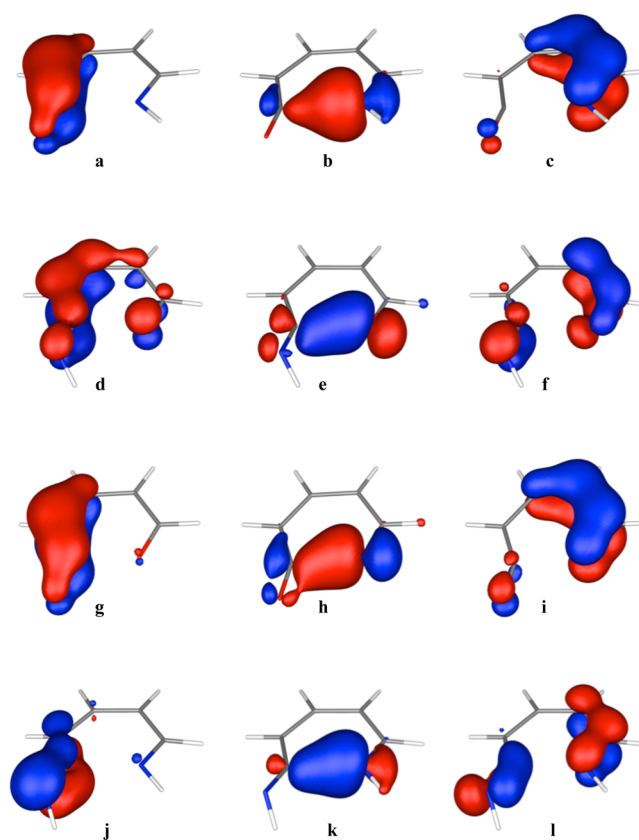


Figure 3. Selected molecular orbitals of the CASSCF-calculated transition structures of the four pseudopericyclic rearrangements. Orbitals in 4a–c belong to $TS_{3 \rightarrow 4}$. Orbitals in 4d–f belong to $TS_{5 \rightarrow 6}$. Orbitals in 4g–i belong to $TS_{7 \rightarrow 8}$. Orbitals in 4j–l belong to $TS_{9 \rightarrow 10}$.

a, the internal π -orbital of the ketenyl moiety can be seen intact, not participating in forming the new bond, as it would be in a pericyclic rearrangement. Similarly, in c of Figure 3, the C6–N7 π -bond (cf. atoms numbered as in Figure 2) can be seen intact and not participating in formation of the new bond.

While it was expected that the $3 \rightarrow 4$ rearrangement would be pseudopericyclic, at least a lesser extent of pseudopericyclic character was anticipated for the other rearrangements. However, this turned out not to be the case. Rearrangements $5 \rightarrow 6$, $7 \rightarrow 8$, and $9 \rightarrow 10$ (Scheme 2) also appear by this method to be pseudopericyclic with two orbital disconnections. This is also demonstrated in Figure 3 that depicts the clear similarity of the active-space orbitals calculated for $TS_{5 \rightarrow 6}$, $TS_{7 \rightarrow 8}$, and $TS_{9 \rightarrow 10}$ with those calculated for $TS_{3 \rightarrow 4}$. While our results confirm those of Rodríguez-Otero et al. with respect to the $7 \rightarrow 8$ rearrangement,¹⁷ they are contradictory with respect to the $5 \rightarrow 6$ electrocyclization which Rodríguez-Otero et al. concluded was pericyclic as opposed to pseudopericyclic.²³

The fact that all four of the above rearrangements appear to be pseudopericyclic implies that the relative nucleophilicity and electrophilicity of the reacting centers are not the only factors that influence pseudopericyclic character in these electrocyclizations. In the [3,3] sigmatropic rearrangement study carried out by Forte et al., involving the $11 \rightarrow 12$ and similar rearrangements,⁷ the electrophilicity and nucleophilicity of the heteroatoms alone provided a satisfactory explanation for the results because the sigmatropic rearrangements analogous to the $5 \rightarrow 6$, $7 \rightarrow 8$, and $9 \rightarrow 10$ ones [i.e., with the 4–5 $\text{C}=\text{C}$ π -bond of the electrocyclization reactants replaced by the fused

cyclopropane ring of the [3,3] sigmatropic rearrangement reactants (cf. Figure 2)] turned out to be pericyclic.⁷ However, in this study, even rearrangement $5 \rightarrow 6$, which has the “worst” combination of reacting substituents, an aldehyde group and a keteniminy ($-\text{CH}=\text{C}=\text{NH}$) group, is pseudopericyclic. Thus, there must be at least one other factor that contributes to the orbital disconnections observed in these pseudopericyclic electrocyclicizations. It is likely that the formation of an allyl system over the cumulene group in the transition structures stabilizes them and contributes to the reactions being pseudopericyclic. An allyl system consisting of the internal π -bond of the cumulene system and the terminal lone-pair orbital can be seen forming in all cases (a, d, g, and j of Figure 3). (MOs showing the corresponding nonbonding and antibonding allyl moieties for $\text{TS}_{3 \rightarrow 4}$, $\text{TS}_{5 \rightarrow 6}$, $\text{TS}_{7 \rightarrow 8}$, and $\text{TS}_{9 \rightarrow 10}$ can be seen in the Supporting Information.)

The $13 \rightarrow 14$ and $15 \rightarrow 16$ rearrangements that have the nitrogen at an internal position (Scheme 4) were studied as a test of this hypothesis. In 13 and 15, the lone pair of electrons in the N_{sp^2} orbital cannot participate in forming a stabilized allyl system, as can the N_{p} and O_{p} lone pairs of electrons on the terminal nitrogen atoms in 5 and 11 and the terminal oxygen atoms in 3 and 7, respectively.

The active-space orbitals of the calculated transition structures $\text{TS}_{13 \rightarrow 14}$ and $\text{TS}_{15 \rightarrow 16}$ (Figure 4), which clearly do

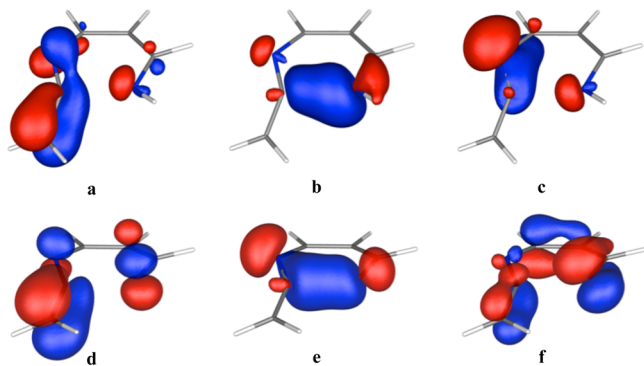


Figure 4. Selected molecular orbitals of the pericyclic reactions. Orbitals 5a–c belong to $\text{TS}_{13 \rightarrow 14}$. Orbitals 5d–f belong to $\text{TS}_{15 \rightarrow 16}$.

not include an allyl system, show that the $13 \rightarrow 14$ and $15 \rightarrow 16$ rearrangements (Scheme 4) are pericyclic. The b and e orbitals of Figure 4 depict the formation of the new σ -bonds and it can be seen that the lone-pair orbitals on the nitrogen atom ($\text{TS}_{13 \rightarrow 14}$) and oxygen atom ($\text{TS}_{15 \rightarrow 16}$) are still overlapping slightly with the two π -orbitals forming the bond. There is a secondary orbital effect from the lone pair similar to the one we proposed for the $1 \rightarrow 2$ rearrangement.⁶ However, it is primarily the π -orbitals forming the new bond, specifically the $\text{N}7-\text{C}6$ and $\text{N}3-\text{C}2$ π -orbitals ($\text{TS}_{13 \rightarrow 14}$) and the $\text{O}7-\text{C}6$ and $\text{N}3-\text{C}2$ π -orbitals ($\text{TS}_{15 \rightarrow 16}$) (see Figure 2 for atom-numbering scheme). On the left-hand side of both b and e of Figure 4, electron density from the inner π -orbitals ($\text{N}3-\text{C}2$) of the cumulene systems can be inferred, which indicates that they participate in formation of the new σ -bonds. Conversely, in a and d of Figure 4, the outer π -orbitals ($\text{C}1-\text{C}2$) of the cumulene systems can be seen intact and not participating in formation of the new σ -bonds. It is a bit more difficult to determine how the orbitals are forming on the right-hand side of orbitals b and e of Figure 4, but there appear to be no orbital disconnections involved. The lone pair is angled slightly

downward, not pointing directly at the central carbon atom of the cumulene system. This also suggests that the $\text{C}-\text{O}$ and $\text{C}-\text{N}$ π -orbitals, not the lone-pair orbitals, are primarily responsible for forming the new σ -bonds. These results run counter to the conclusion of Rodríguez-Otero et al. that the $15 \rightarrow 16$ rearrangement is pseudopericyclic;²³ for completeness, we appear to be the first to study the corresponding $13 \rightarrow 14$ rearrangement computationally.

Comparisons of the geometry of the six transition structures also supports the conclusion that $\text{TS}_{3 \rightarrow 4}$, $\text{TS}_{5 \rightarrow 6}$, $\text{TS}_{7 \rightarrow 8}$, and $\text{TS}_{9 \rightarrow 10}$ are pseudopericyclic, whereas $\text{TS}_{13 \rightarrow 14}$ and $\text{TS}_{15 \rightarrow 16}$ are pericyclic. Pertinent dihedral angles of all six transition structures are listed in Table 1. Structures $\text{TS}_{3 \rightarrow 4}$, $\text{TS}_{5 \rightarrow 6}$,

Table 1. Dihedral Angles (deg) for All Calculated Transition Structures^a

dihedral angle (deg)	transition structure					
	$\text{TS}_{3 \rightarrow 4}$	$\text{TS}_{5 \rightarrow 6}$	$\text{TS}_{7 \rightarrow 8}$	$\text{TS}_{9 \rightarrow 10}$	$\text{TS}_{13 \rightarrow 14}$	$\text{TS}_{15 \rightarrow 16}$
2–3–4–5	−0.03	7.78	0.00	6.66	−27.88	−21.58
3–4–5–6	−0.04	4.77	0.00	1.46	−3.55	−3.32
4–5–6–7	0.03	−9.32	0.00	−8.85	18.02	13.23

^aThe numbers in the leftmost column correspond to the numbers assigned to atoms in Figure 2.

$\text{TS}_{7 \rightarrow 8}$, and $\text{TS}_{9 \rightarrow 10}$ are relatively planar, which is expected of pseudopericyclic reactions. All dihedral angles for $\text{TS}_{7 \rightarrow 8}$ are 0.00° , so it is completely planar. The values are slightly higher in $\text{TS}_{3 \rightarrow 4}$, but only by 0.03 or 0.04° , so $\text{TS}_{3 \rightarrow 4}$ is also almost completely planar. The dihedral angles are higher for $\text{TS}_{5 \rightarrow 6}$ and $\text{TS}_{9 \rightarrow 10}$, but still quite low. A planar geometry facilitates the overlap of the orbitals orthogonal to bonding orbitals in the reactant. If the π -orbitals between $\text{C}2-\text{C}3$ and $\text{C}6-\text{N}7$ were used, twisting would be necessary for them to overlap, but no such twisting is evident. No dihedral angle for the first four transition structures is greater than 9.32° . On the other hand, $\text{TS}_{13 \rightarrow 14}$ and $\text{TS}_{15 \rightarrow 16}$ have dihedral angles as great as 27.88° . These transition structures are much less planar, which is congruent with them being pericyclic.

The optimized transition structures for all six rearrangements studied here are shown in Figure 5. These representations are useful for visualizing both the geometries and the vectors depicting the normal mode of vibration for the imaginary frequency for the calculated structures in each case. All six transition structures clearly show the formation of the new σ -bond. In $\text{TS}_{13 \rightarrow 14}$, the vector indicating the motion of the hydrogen atom on the imine moiety demonstrates a slight upward motion, close to a twist. This likely indicates rotation of the $\text{C}-\text{N}$ π -orbitals to form the new σ -bond, and is similar to that of the imine hydrogen of $\text{TS}_{1 \rightarrow 2}$, which was previously determined by us to be essentially pericyclic.⁶ Such rotation cannot be seen in $\text{TS}_{9 \rightarrow 10}$, the corresponding pseudopericyclic reaction. The vector on the hydrogen of the imine moiety in $\text{TS}_{9 \rightarrow 10}$ demonstrates only an inward, in-plane motion, indicating that the π -orbitals do not rotate and the lone-pair orbital is likely involved in the formation of the new σ -bond. [See the Supporting Information for alternative three-dimensional representations of transition structures and imaginary frequency normal mode vectors.]

Calculated energies of activation for the $3 \rightarrow 4$, $5 \rightarrow 6$, $7 \rightarrow 8$, and $9 \rightarrow 10$ rearrangements also support their pseudopericyclic character. As shown in Table 2 (first four data rows and

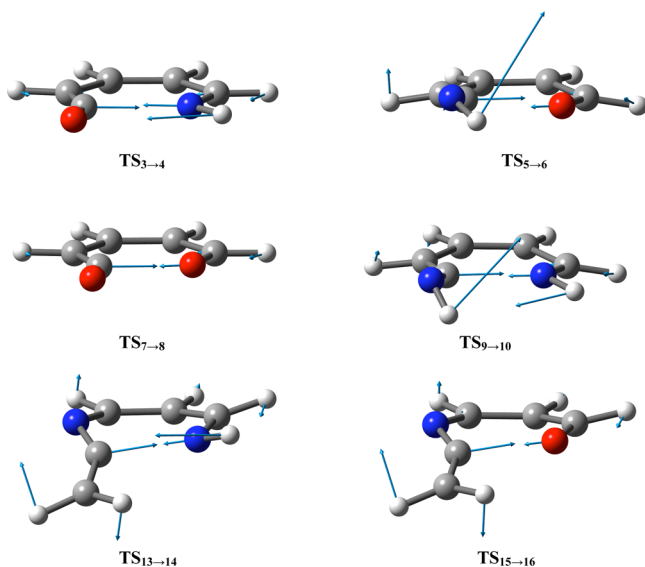


Figure 5. Calculated transition structures including vectors (blue arrows) illustrating the normal mode of vibration corresponding to the single calculated imaginary frequencies for $\text{TS}_{3\rightarrow 4}$, $\text{TS}_{5\rightarrow 6}$, $\text{TS}_{7\rightarrow 8}$, $\text{TS}_{9\rightarrow 10}$, $\text{TS}_{13\rightarrow 14}$, and $\text{TS}_{15\rightarrow 16}$ (cf. Schemes 2 and 4). Red = oxygen, blue = nitrogen, gray = carbon, white = hydrogen. All forming σ -bonds can be inferred (opposing blue arrows). The pseudopericyclic transition structures (top four) are much more planar than the pericyclic ones (bottom two).

Table 2. Zero-Point Corrected Activation Energies at the CASSCF/6-31G*//CASSCF/6-31G* and CASPT2/6-31G*//CASSCF/6-31G* Levels for the Six Calculated Electrocyclic Rearrangements

electrocyclic rearrangement	CASSCF//CASSCF E_a (kcal/mol)	CASPT2//CASSCF E_a (kcal/mol)
3 \rightarrow 4	1.49	-5.69
5 \rightarrow 6	13.81	0.43
7 \rightarrow 8	0.11	-8.56
9 \rightarrow 10	13.89	1.82
13 \rightarrow 14	20.50	8.00
15 \rightarrow 16	20.61	7.42

first data column), the CASSCF/6-31G*//CASSCF/6-31G*-calculated zero-point corrected energies are rather low, which is alleged to be typical of pseudopericyclic rearrangements.²⁴ The two lowest activation energies (1.49 and 0.11 kcal/mol) involve the more electrophilic ketenyl cumulene moiety, whereas the higher ones (13.81 and 13.89 kcal/mol) involve the less electrophilic keteniminyl cumulene moiety, as one might expect. One might also expect a preference for the more nucleophilic iminyl group involved in the 3 \rightarrow 4 rearrangement vs the less nucleophilic carbonyl group involved in the 7 \rightarrow 8 rearrangement; however, the CASSCF/6-31G*//CASSCF/6-31G* activation energies run counter to this. Likewise, one might expect the 5 \rightarrow 6 rearrangement to have a lower energy of activation than the 9 \rightarrow 10 rearrangement, and it does but with a negligible activation energy difference of only 0.08 kcal/mol (Table 2, data rows 2 and 4 and data column 1). However, when dynamic electron correlation was included by performing CASPT2 single-point calculations, with the same basis set, on the CASSCF wave functions (i.e., from CASPT2/6-31G*//CASSCF/6-31G* calculations), the activation energy difference is much greater (1.39 kcal/mol) and in favor of the 5 \rightarrow 6

rearrangement as expected (Table 2, data rows 2 and 4, data column 2). Unfortunately, performing CASPT2 calculations on both the 3 \rightarrow 4 and 7 \rightarrow 8 rearrangements yielded nonviable negative activation energies (Table 2, data rows 1 and 3, data column 2). It seems that the inaccuracy in calculated CASSCF/6-31G* activation energy values is greater than the magnitude of the CASPT2 “corrections” in these cases. [Table S1 in the Supporting Information also gives the activation energies for the CASPT2-corrected activation energies for the 3 \rightarrow 4 and 7 \rightarrow 8 rearrangements using alternative basis sets (6-31G**, ANO-RCC-VDZP, and cc-pVDZ0). As can be seen, the choice of basis set had insufficient influence on the activation energies for these two rearrangements for them to be positive.] Nonetheless, as shown in Table 2, the CASPT2/6-31G*//CASSCF/6-31G* energies remain in the same relative order as the CASSCF/6-31G*//CASSCF/6-31G* energy ones.

Finally, it can be seen that the calculated activation energies for the 13 \rightarrow 14 and 15 \rightarrow 16 pericyclic rearrangements have much higher relative activation energies than their pseudopericyclic counterparts (Table 2, first and second data columns), as expected, and with no discernible preference for the stronger nucleophilicity of the iminyl nitrogen atom in $\text{TS}_{13\rightarrow 14}$ vs the weaker nucleophilicity of the carbonyl oxygen atom in $\text{TS}_{15\rightarrow 16}$ (Table 2, last two entries in the first and second data columns). This later observation is consistent with it being primarily the π -bond of the iminyl and carbonyl moieties, as opposed to the nitrogen and oxygen atom lone pairs, being involved in these transition structures. [Both CASPT2/6-31G*//CASSCF/6-31G* and CASSCF/6-31G*//CASSCF/6-31G* calculations also demonstrate that the 5 \rightarrow 6, 7 \rightarrow 8, 9 \rightarrow 10, 13 \rightarrow 14, and 15 \rightarrow 16 rearrangements are all exothermic; the 3 \rightarrow 4 rearrangement is almost certainly exothermic as well, though it could not be calculated at this level since a (12,10)CASSCF/6-31G* structure for 4 proved to be elusive.³¹]

The geometries of the transition structures also appear to correlate well with the calculated energies of activation. The most planar transition structure, $\text{TS}_{7\rightarrow 8}$ (cf. Table 1), is associated with the lowest CASSCF/6-31G* activation energy and pseudopericyclic behavior, while the least planar transition structure, $\text{TS}_{15\rightarrow 16}$, is associated with the highest activation energy and pericyclic character. The other transition structures also range from planar to less planar in the same order that their associated activation energies range from lowest to highest.

SUMMARY AND CONCLUSIONS

This study examined six electrocyclic rearrangements (3 \rightarrow 4, 5 \rightarrow 6, 7 \rightarrow 8, 9 \rightarrow 10, 13 \rightarrow 14, and 15 \rightarrow 16) at the CASSCF/6-31G* level to determine whether any were pseudopericyclic, and if so, whether degrees of pseudopericyclic character existed among them. This was accomplished primarily by examining the localized active space MOs to see which were used to form the new σ -bonds, as well as through an examination of transition-state geometries (deviations from planarity) and activation energies.

Based on the active-space MOs of the optimized transition structures shown in Figure 3, it is concluded that rearrangements 3 \rightarrow 4, 5 \rightarrow 6, 7 \rightarrow 8, and 9 \rightarrow 10 are pseudopericyclic. The lone pair on the nitrogen or oxygen atom at site 7 (Figure 2, structure a) participates in forming the new σ -bond in every case, as does the outer π -orbital of the cumulene system. So, each is pseudopericyclic with two orbital disconnections. On the other hand, rearrangements 13 \rightarrow 14 and 15 \rightarrow 16 are

pericyclic. This conclusion is supported by the nearly planar ring geometries for $\text{TS}_{3\rightarrow 4}$, $\text{TS}_{5\rightarrow 6}$, $\text{TS}_{7\rightarrow 8}$, and $\text{TS}_{9\rightarrow 10}$ vs the decidedly nonplanar geometries for $\text{TS}_{13\rightarrow 14}$ and $\text{TS}_{15\rightarrow 16}$ (Table 1) and the relatively low activation energies for the $3 \rightarrow 4$, $5 \rightarrow 6$, $7 \rightarrow 8$, and $9 \rightarrow 10$ rearrangements vs the much higher activation energies for the $13 \rightarrow 14$ and $15 \rightarrow 16$ rearrangements (Table 2).

These results confirmed those of others in the $3 \rightarrow 4$ ²⁵ and $7 \rightarrow 8$ ^{17,24} rearrangements, but in the case of the $5 \rightarrow 6$ rearrangement our finding that it is pseudopericyclic clashes with the earlier conclusion, based on DFT calculations, that it was pericyclic.²³ Likewise, our finding that the $15 \rightarrow 16$ rearrangement is pericyclic clashes with the previous conclusion that it “can definitely be classified as pseudopericyclic”.²³

As mentioned above, the $1 \rightarrow 2$ electrocyclization was previously found by us to be essentially pericyclic with the nitrogen lone-pair orbital playing only a secondary role.⁶ Yet the similar $3 \rightarrow 4$, $5 \rightarrow 6$, $7 \rightarrow 8$, and $9 \rightarrow 10$ rearrangements have now all been shown to be pseudopericyclic. It is likely that this is at least partially a consequence of the presence in the **3**, **5**, **7**, and **9** reactants of not only a nucleophilic heteroatom at position 7 (Figure 2, structure a) but also an electronegative heteroatom in position 1 that increases the electrophilicity of carbon 2 (Figure 2, structure a). This should strengthen the bond that can be formed at the orbital disconnection sites (2 and 7 of Figure 2, structure a) in the case of a pseudopericyclic transition structure.

However, if the presence of heteroatoms in the 1,2,4,6-heptatetraene moiety (cf. Figure 2a) was reason enough for the $3 \rightarrow 4$, $5 \rightarrow 6$, $7 \rightarrow 8$, and $9 \rightarrow 10$ electrocyclizations to be pseudopericyclic, then the $13 \rightarrow 14$, and $15 \rightarrow 16$ electrocyclizations should likewise be pseudopericyclic. The fact that they turn out to be pericyclic instead, with the role of the nitrogen lone pair of electrons restricted to a secondary role at best, is apparently due to lack of their ability to form a stabilizing allyl system in the transition structures, an ability afforded the other rearrangements by the presence of a lone pair of electrons on the cumulene terminal nitrogen or oxygen atoms. Thus, the presence of heteroatoms is a necessary but not sufficient condition for pseudopericyclicity in these cases.

Finally, we conclude that the reason that the $3 \rightarrow 4$, $5 \rightarrow 6$, $7 \rightarrow 8$, and $9 \rightarrow 10$ electrocyclizations all appear to be pseudopericyclic whereas the $11 \rightarrow 12$ [3,3] sigmatropic rearrangement is the only member of its heteroatom class to be pseudopericyclic⁷ is due to the fact that electrocyclic transition structures are inherently more planar than [3,3] sigmatropic ones, which, of course, prefer chair or boat conformations. Indeed, the geometry of the only pseudopericyclic [3,3] sigmatropic transition structure ($\text{TS}_{11\rightarrow 12}$) was unusual for a Cope-type rearrangement in having a substantially planar six-membered ring conformation, whereas all the other heteroatom combinations (cf. ref 7) have boat-shaped conformations. Thus, only the most advantageous nucleophilic/electrophilic combination of reacting centers is apparently adequate for pseudopericyclicity in that case.

■ ASSOCIATED CONTENT

Supporting Information

The Supporting Information is available free of charge on the ACS Publications website at DOI: 10.1021/acs.joc.5b02223.

Complete ref 27. (12,10)CASSCF/6-31G* optimized geometries for all stationary points found, including

imaginary frequency normal mode vectors for the transition structures. All active-space MOs for **3**, **5–10**, **13–16**, $\text{TS}_{3\rightarrow 4}$, $\text{TS}_{5\rightarrow 6}$, $\text{TS}_{7\rightarrow 8}$, $\text{TS}_{9\rightarrow 10}$, $\text{TS}_{13\rightarrow 14}$, and $\text{TS}_{15\rightarrow 16}$. Table of CASPT2//CASSCF activation energies using other basis sets (PDF)

■ AUTHOR INFORMATION

Corresponding Author

*E-mail: duncan@lclark.edu

Notes

The authors declare no competing financial interest.

[†]I.R.B., C.A.S., and H.W.K. were Lewis & Clark College undergraduate students at the time this work was carried out.

■ ACKNOWLEDGMENTS

Support for this work from the John S. Rogers Science Research Program of Lewis & Clark College is appreciated. We especially thank Mr. Chris Stevens, former Director of Network and Technical Services at Lewis & Clark, for his tireless technical assistance and Dr. David Hrovat of the University of North Texas for his extremely helpful advice in performing calculations over the past 20 years. In addition, I.R.B. thanks former students Lila Forte and Marie C. Lafortune for their valuable mentoring.

■ REFERENCES

- (1) (a) Houk, K. N.; González, J.; Li, Y. *Acc. Chem. Res.* **1995**, *28*, 81–90.
- (2) Anslyn, E. V.; Dougherty, D. A. *Modern Physical Organic Chemistry*; University Science Books: Sausalito, CA, 2006; p 877.
- (3) (a) Greer, E. M.; Cosgriff, C. V. *Annu. Rep. Prog. Chem., Sect. B: Org. Chem.* **2013**, *109*, 328–350. See also previous yearly reports from 1980. (b) Shevelev, S. A.; Starosotnikov, A. M. *Chem. Heterocycl. Compd.* **2013**, *49*, 92–115. (c) Lobo, A. M.; Prabhakar, S. *Pure Appl. Chem.* **1997**, *69*, 547–552. (d) Ylijoki, K. E. O.; Stryker, J. M. *Chem. Rev.* **2013**, *113*, 2244–2266. (e) Hutters, A. D.; Garg, N. K. *Chem. - Eur. J.* **2010**, *16*, 8586–8595. (f) Hardin Narayan, A. R.; Simmons, E. M.; Sarpong, R. *Eur. J. Org. Chem.* **2010**, *19*, 3553–3567. (g) Arns, S.; Barriault, L. *Chem. Commun.* **2007**, 2211–2221. (h) Poulin, J.; Grise-Bard, C. M.; Barriault, L. *Chem. Soc. Rev.* **2009**, *38*, 3092–3101.
- (4) Woodward, R.; Hoffmann, R. *The Conservation of Orbital Symmetry*; Academic Press: New York, 1970.
- (5) Ross, J. A.; Seiders, R. P.; Lemal, D. M. *J. Am. Chem. Soc.* **1976**, *98*, 4325–4327.
- (6) Duncan, J. A.; Calkins, D. E. G.; Chavarha, M. *J. Am. Chem. Soc.* **2008**, *130*, 6740–6748.
- (7) Forte, L.; Lafortune, M. C.; Bierzynski, I. R.; Duncan, J. A. *J. Am. Chem. Soc.* **2010**, *132*, 2196–2201.
- (8) Takao, K.; Munakata, R.; Tadano, K. *Chem. Rev.* **2005**, *105*, 4779–4807.
- (9) Ansari, F. L.; Qureshi, R.; Qureshi, M. L.; *Electrocyclic Reactions: From Fundamentals to Research*; Wiley-VCH: Weinheim, 1999; Vol. 1.
- (10) Tietze, L.; Brasche, G.; Gericke, K. M.; *Domino Reactions in Organic Synthesis*. Wiley-VCH: Weinheim, 2006.
- (11) Schleyer, P. V.; Maerker, C.; Dransfeld, A.; Jiao, H. J.; Hommes, N. *J. Am. Chem. Soc.* **1996**, *118*, 6317–6318.
- (12) Herges, R.; Papafilippopoulos, A. *Angew. Chem., Int. Ed.* **2001**, *40*, 4671–4674.
- (13) Matito, E.; Poater, J.; Duran, M.; Solá, M. *ChemPhysChem* **2006**, *7*, 111–113.
- (14) Rodríguez-Otero, J.; Cabaleiro-Lago, E. *Angew. Chem., Int. Ed.* **2002**, *41*, 1147–1150.
- (15) de Lera, A. R.; Alvarez, R.; Lecea, B.; Torrado, A.; Cossío, F. P. *Angew. Chem., Int. Ed.* **2001**, *40*, 557–561.
- (16) de Lera, A. R.; Cossío, F. P. *Angew. Chem., Int. Ed.* **2002**, *41*, 1150–1152.

- (17) Rodríguez-Otero, J.; Cabaleiro-Lago, E. *Chem. - Eur. J.* **2003**, *9*, 1837–1843.
- (18) Chamorro, E. E.; Notario, R. *J. Phys. Chem. A* **2004**, *108*, 4099–4104.
- (19) Chamorro, E. E.; Notario, R. *J. Phys. Chem. B* **2005**, *109*, 7594–7595.
- (20) Matito, E.; Solà, M.; Duran, M.; Poater, J. *J. Phys. Chem. B* **2005**, *109*, 7591–7593.
- (21) Lee, P. S.; Sakai, S.; Hörstermann, P.; Roth, W. R.; Kallel, E. A.; Houk, K. N. *J. Am. Chem. Soc.* **2003**, *125*, 5839–5848.
- (22) Pham, H. V.; Houk, K. N. *J. Org. Chem.* **2014**, *79*, 8968–8976.
- (23) Cabaleiro-Lago, E. M.; Rodríguez-Otero, J.; García-López, R. M.; Peña-Gallego, A.; Hermida-Ramón, J. M. *Chem. - Eur. J.* **2005**, *11*, 5966–5974.
- (24) Birney, D. M. *J. Org. Chem.* **1996**, *61*, 243–251.
- (25) Cabaleiro-Lago, E. M.; Rodríguez-Otero, J.; Varela-Varela, S. M.; Peña-Gallego, A.; Hermida-Ramón, J. M. *J. Org. Chem.* **2005**, *70*, 3921–3928.
- (26) Ji, H.; Xu, X.; Ham, S.; Hammad, L. A.; Birney, D. M. *J. Am. Chem. Soc.* **2009**, *131*, 528–537 and references cited therein.
- (27) (a) Frisch, M. J.; et al. *Gaussian 03, Revision D.01*; Gaussian, Inc.: Wallingford, CT, 2004. (b) Frisch, M. J.; et al. *Gaussian 09, Revision B.01*; Gaussian, Inc.: Wallingford, CT, 2010.
- (28) Molcas 7.4: Karlström, G.; Lindh, R.; Malmqvist, P.-Å.; Roos, B. O.; Ryde, U.; Veryazov, V.; Widmark, P.-O.; Cossi, M.; Schimmelpfennig, B.; Neogrady, P.; Seijo, L. *Comput. Mater. Sci.* **2003**, *28*, 222–239.
- (29) Bode, B. M.; Gordon, M. S. *J. Mol. Graphics Modell.* **1998**, *16*, 133–138.
- (30) Dennington, R.; Keith, T.; Millam, J. *GaussView, Version 5*; Semichem, Inc.: Shawnee Mission, KS, 2009.
- (31) It proved too difficult to simultaneously obtain one lone-pair orbital on the oxygen atom and the correct, new (i.e., not in reactant) σ and σ^* active-space orbitals of structure 4.